Transient receptor potential canonical 3/5 attenuate endothelial damage-induced neointima formation without affecting endothelial cell proliferation

Wenjun Zeng,[1,2] Bei Liu,[3] Lixia Yang,[3] Ruiwei Guo[3,4]

[1]Department of Geratology, The first People's Hospital of Yunnan Province, Kunming, Yunnan, [2]Kunming Medical University, Kunming, Yunnan; [3]Department of Cardiology, 920th Hospital of Joint Logistics Support Force, PLA, Kunming, Yunnan; [4]922th Hospital of Joint Logistics Support Force, PLA, Hengyang, Hunan, China

ABSTRACT

Store-operated calcium channels (SOCCs) are involved in the process of cell proliferation; however, their expression levels differ among cell types and information on their effects in different cells is lacking. This study aimed to compare the differing effects of SOCCs on the proliferation of vascular smooth muscle cells (VSMCs) and vascular endothelial cells (VECs), and the repair ability of SOCC after vascular endothelial injury. Rat primary coronary VSMCs and VECs were cultured *in vitro* and expression levels of SOCC molecules were detected by western blotting and quantitative polymerase chain reaction. Various molecules were selected and transfected into VSMCs and VECs using an adenovirus vector, and cell proliferation, the cell cycle, and intracellular Ca^{2+} were then detected. We also established a rat carotid artery endothelial injury model to verify the results of the *in vitro* experiments. Expression levels of transient receptor potential canonical (TRPC) 3 and TRPC5 were higher in VSMCs than in VECs. Silencing TRPC3/5 significantly inhibited cell proliferation and Ca2+ influx in VSMCs, but not in VECs. Silencing TRPC3/5 after rat carotid artery endothelial injury inhibited neointima formation, with a better reparative effect on the endothelial cell layer than rapamycin. TRPC3/5 participates in the proliferation of VSMCs *via* SOCCs, and silencing its expression inhibits the formation of neointima after endothelial injury. However, this effect was not significant in VECs, suggesting that other compensatory pathways may have emerged.

Key words: store-operated calcium channels; cell proliferation; in-stent restenosis.

Correspondence: Ruiwei Guo, Department of Cardiology, 920th Hospital of Joint Logistics Support Force, PLA, 212 Daguan Road, Kunming, Yunnan 650032, China. E-mail: grw771210@163.com

Contributions: RG, study concept and design; WZ, BL, LY, data analysis and interpretation; WZ, manuscript original drafting. All authors read and approved the final version of the manuscript and agreed to be accountable for all aspects of the work.

Conflict of interest: the authors declare no competing interests and all authors confirm accuracy.

Ethical approval: all procedures complied with the Guide for the care and use of laboratory animals (NIH Publication No. 8-23, revised 1996) and were approved by the Animal Ethics Committee of the 920th Hospital of Joint Logistics Support Force Animal Center (Approval no. 2021046).

Availability of data and materials: the datasets used and/or analyzed during the current study are available upon reasonable request from the corresponding author.

Funding: this study was supported by grant from the Technology Department Kunming Medical University joint special key project of Yunnan Provincial Science (no. 202101AY070001-030) and grant from Yunnan Provincial Department of Science and Technology Basic Research Program (no. 202501AU070016).

Introduction

Coronary heart disease is a global health problem. The main current treatment is percutaneous coronary intervention (PCI), but this procedure is associated with complications such as in-stent restenosis and thrombosis. Although the introduction of drug-eluting stents has significantly reduced the incidence of in-stent restenosis (<10%) and improved both mortality and clinical symptoms in patients with coronary heart disease, limitations remain, and the risk of major adverse cardiovascular events after surgery persists.[1,2]

Drug-eluting stents inhibit excessive neointimal hyperplasia after stent implantation and reduce in-stent restenosis by locally releasing coating drugs such as rapamycin or paclitaxel. However, rapamycin is a broad-spectrum anti-proliferative agent that exerts non-selective effects. It not only suppresses the proliferation of vascular smooth muscle cells (VSMCs) but also delays repair of the layer of vascular endothelial cells (VECs).[3] An intact endothelial cell layer is essential for inhibiting neointima formation. Thus, the use of drug-eluting stents prevents rapid re-endothelialization, delays arterial healing, and leaves the stent surface exposed within the vascular lumen, which may lead to stent thrombosis.[4] Consequently, patients are required to take dual antiplatelet therapy for at least one year after stent implantation, which increases the risk of bleeding. Store-operated calcium channels (SOCCs) play a crucial role in cell proliferation. SOCCs include stromal interaction molecule (STIM), calcium release-activated calcium channel (Orai), transient receptor potential canonical (TRPC), and the Na^+/Ca^{2+} exchanger (NCX). In the resting state, STIM1 is located in the endoplasmic reticulum (ER), while Orai1 resides in the plasma membrane. When the ER Ca^{2+} concentration decreases, STIM1 is activated and binds to Orai1 on the plasma membrane, leading to SOCC opening, calcium release, and activation of the calcium-release-activated Ca^{2+} current (ICRAC). The intracellular Ca^{2+} concentration then gradually increases, replenishing cytoplasmic levels and refilling the calcium pool until saturation is reached, at which point Ca^{2+} influx ceases, and the resting state is restored.[5,6] To date, no drugs have been identified that can differentially regulate VSMCs and VECs. Most research has focused on degrading the adhesive material between the stent and the drug, or on developing fully biodegradable stents, whereas few studies have explored alternatives to the coating drugs.[7]

In this study, we aimed at identifying SOCC molecules that can inhibit VSMC proliferation without affecting VEC proliferation. We also investigated the distinct regulatory roles of SOCC-related molecules in different cell types, as well as their differential mechanisms in regulating VSMC and VEC proliferation. The findings of this study may help reduce the required duration of dual antiplatelet therapy after PCI and provide a new direction for the development of drug-eluting stent coatings. To our knowledge, this is the first study to systematically compare the differential roles of TRPC3 and TRPC5 in vascular smooth muscle and endothelial cells using both *in vitro* and *in vivo* models. Previous studies have mainly explored SOCC functions in a single cell type, whereas our findings reveal that selective inhibition of TRPC3/5 can suppress smooth muscle proliferation without impairing endothelial repair. This provides a novel mechanistic basis for developing next-generation drug-eluting stents that promote endothelial healing while preventing neointimal hyperplasia.

Materials and Methods

Cell culture

Rat coronary artery VSMCs and VECs (Procell, China) were cultured as previously described in Dulbecco's Modified Eagle's Medium/F12 (DMEM/F12; Hyclone, Logan, UT, USA) supplemented with 10% fetal bovine serum (FBS; Hyclone), at 37°C in a 5% CO_2 incubator.[8,9] VSMCs and VECs at passages 8-10 were used for the experiments.

Western blot analysis

Proteins were extracted from VSMCs and VECs using lysis buffer. Western blotting was performed with the following antibodies: rabbit monoclonal anti-STIM1 (ab108994; 1:1000), rabbit polyclonal anti-STIM2 (ab59342; 1:1000), mouse monoclonal anti-Orai1 (ab175040; 1:1000), rabbit monoclonal anti-Orai2 (ab180146; 1:1000), mouse monoclonal anti-Orai3 (MA5-15778; 1:1000), rabbit monoclonal anti-TRPC1 (ab192031; 1:1000), mouse monoclonal anti-TRPC3 (sc-514670; 1:500), goat polyclonal anti-TRPC4 (ab111841; 1:1000), mouse monoclonal anti-TRPC5 (ab240872; 1:1000), rabbit polyclonal anti-TRPC6 (ab101622; 1:1000), rabbit monoclonal anti-NCX1 (ab177952; 1:2000), and mouse monoclonal anti-NCX2 (sc-515768; 1:500). All antibodies were obtained from Abcam (Cambridge, MA, USA) or Santa Cruz Biotechnology (sc; Santa Cruz, CA, USA). Densitometric analysis of the gels was performed using ImageJ software.

Table 1. Primers sequences.

Gene	*Forward (5'-3')*	*Reverse (5'-3')*
GAPDH	CTGGAGAAACCTGCCAAGTATG	GGTGGAAGAATGGGAGTTGCT
NCX1	AGGTTCTGTTTGCCTTCGTCC	CACTGAGGTTCCAAGAGCGAC
NCX2	GGGCACTGAGGTCCCAGGCGAGCT	CAGCAGCCTCACGAAGAAGTGCTC
STIM1	GGATCTCAGAGGGATTTGACCC	CATTGGAAGACGTGGCATTGA
STIM2	GAACAACACTTCCCAGGATAGCA	CAACAACCTCCAACGCCAAT
TRPC1	AAAAAGGACAGCCTCAGACATTC	GCACTAAGTTCAAACGCTCTCAG
TRPC3	AGCATTCTCAATCAGCCAACA	CCGTCGCTTGGCTCTTATCTT
TRPC4	CAGATGTGGGATGGCGGACT	CAATTGCGAATAAAGCCTCTGC
TRPC5	TGTGTGGAGTGTGTGTCCAG	GCCGGAATGCTGTGAGGATA
TRPC6	CAGGACTATCTGCTGATGGACGA	GCACCACTGGGATGTTGCC
Orai1	AAAGCCTCCAGCCGAACCT	AAAAGCAGCGTCCCGATGAC
Orai2	AAGGGCATGGATTACCGAGACTG	CTGAGGGTACTGGTACTTGGTCTC
Orai3	CACTTCTGCTCTGCTGTCGG	TCAATATGGGGCAGCAGACA

RNA isolation and RT-qPCR

Total RNA was extracted using TRIzol reagent (Invitrogen, Waltham, MA, USA) according to the manufacturer's instructions. RNA was reverse-transcribed into cDNA, which was subsequently amplified using SYBR Green I-based quantitative RT-PCR. Primer sequences are listed in Table 1. PCR amplification was performed for 40 cycles with the following profile: denaturation at 95°C for 10 s, annealing at 60°C for 32 s, and extension at 60°C for 32 s.

Flow cytometry

Cell cycle distribution was assessed by flow cytometry. Briefly, VSMCs and VECs were harvested by trypsinization, washed twice with phosphate-buffered saline (PBS), and fixed in 70% cold ethanol at 4°C overnight. After fixation, cells were washed again with PBS and incubated with RNase A (100 µg/mL) at 37°C for 30 min to remove RNA. Cells were then stained with propidium iodide (PI, 50 µg/mL) for 30 min at room temperature in the dark. Each sample was resuspended in 0.5 mL PI staining solution and analyzed using a FACScan flow cytometer (BD Biosciences, Franklin Lakes, NJ, USA), with at least 10,000 events collected per sample. Each condition was tested in triplicate. Cell-cycle phases (G_0/G_1, S, G_2/M) were determined using ModFit LT software (Verity Software House, Topsham, ME, USA).

Measurement of intracellular free Ca^{2+}

VSMCs and VECs were incubated with 5 µmol/L Fura-2/AM. Intracellular Ca^{2+} was measured as the ratio of fluorescence intensity at 340 nm/380 nm. SOCC-mediated calcium influx was stimulated with 1 µM thapsigargin (TG) during the transition from Ca^{2+}-free conditions to 2 mM Ca^{2+}.

Endothelial injury model

Male Sprague-Dawley (SD) rats (weighing ~300 g) were anesthetized by intraperitoneal injection of 1 mL/100 g of 0.3% sodium pentobarbital, and a midline neck incision was made to expose the left common carotid artery and the internal and external carotid arteries. The distal end of the external carotid artery was ligated with 6-0 sutures and clamped with a micro-hemostatic clip. The left common carotid and internal carotid arteries were clamped, and a vertical incision was made in the distal external carotid artery to approximately one-third to one-half of the vessel circumference. A 2.0 F balloon catheter (Cordis, Miami Lakes, FL, USA) was inserted into the common carotid artery, inflated to 2 atm, and withdrawn three times to denude the endothelium. A total of 10 µL of adenovirus or rapamycin solution (NSC, sh-TRPC3, sh-TRPC5, rapamycin; n=6) was then injected into the incision site with a microsyringe for 15 min. At 7 or 14 days post-arteriotomy, rats were euthanized with an overdose of sodium pentobarbital (150 mg/kg, intraperitoneally). Carotid arteries were harvested and stained with hematoxylin and eosin (see below). All procedures complied with the Guide for the Care and Use of Laboratory Animals (NIH Publication No. 85-23, revised 1996) and were approved by the Animal Ethics Committee of the 920th Hospital of Joint Logistics Support Force Animal Center (Approval no. 2021046).

Transfection of adenoviral vectors

Approximately 1×10^5 cells were seeded per well in 6-well plates (40-60% confluency the next day). The virus volume (µL) was calculated as: number of cells × MOI / titer (TU/mL) × 1000. With MOI = 100, 2.5 µL of adenovirus was added per well. After infection, cells were mixed and cultured. At 12 h post-infection, cells remained healthy and showed no adverse effects. The medium was replaced with fresh culture medium at 24 h, and cells were further cultured. At 48 h, cells were observed and photographed under a fluorescence microscope.

Hematoxylin and eosin staining

Fresh rat carotid artery tissues were fixed in 10% neutral buffered formalin for at least 24 h. Samples were dehydrated through graded ethanol, cleared in xylene, embedded in paraffin, and sectioned at the appropriate thickness. Sections were sequentially stained with hematoxylin and eosin, dehydrated, and mounted for microscopic examination.

Immunohistochemistry

Paraffin-embedded tissue sections were dewaxed, rehydrated, and treated with 3% hydrogen peroxide at room temperature for 25 min in the dark to quench endogenous peroxidase. After three rinses in PBS (pH 7.4), sections were blocked with 3% bovine serum albumin (BSA) for 30 min. The primary antibody was anti-von Willebrand factor (vWF; rabbit monoclonal, ab287962; 1:50). Negative controls omitted the primary antibody; positive controls used rat vascular tissue known to express vWF. Sections were incubated overnight at 4°C in a humidified chamber. After washing with PBS, slides were incubated with goat anti-rabbit IgG secondary antibody conjugated to horseradish peroxidase (HRP; ab6721; 1:1000) for 50 min at room temperature. Immunoreactivity was visualized using 3,3′-diaminobenzidine (DAB), and nuclei were counterstained with hematoxylin. Slides were dehydrated, cleared, mounted, and examined under an Olympus BX53 microscope at 20× and 40× magnifications. At least five randomly selected fields per sample were analyzed. Immunolabeling intensity and distribution were semi-quantitatively assessed with ImageJ, and results were averaged across three independent replicates.

Immunofluorescence

Paraffin sections were dewaxed and blocked with BSA for 30 min. After removal of the blocking solution, primary anti-vWF antibodies were applied, then the sections were washed three times for 5 min each in PBS (pH 7.4) with gentle shaking and incubated with Cy3-labeled secondary antibodies for 50 min at room temperature. Slides were washed again, stained with DAPI solution for 10 min in the dark, rinsed, and treated with an autofluorescence quencher for 5 min before mounting. Observations were performed under a fluorescence microscope. DAPI-stained nuclei appeared blue (UV excitation 330-380 nm, emission 420 nm) and Cy3 signals appeared red (excitation 510-560 nm, emission 590 nm).

Transmission electron microscopy

Carotid artery specimens (approximately 1 mm^3) from each group were excised at 14 days post-injury and immediately fixed in 2.5% glutaraldehyde in 0.1 M phosphate buffer (pH 7.4) at 4°C for 24 h. After three rinses in phosphate buffer, tissues were post-fixed in 1% osmium tetroxide for 1 h, dehydrated in graded ethanol and acetone, and embedded in epoxy resin. Ultrathin 70 nm-thick sections were cut with an ultramicrotome, mounted on copper grids, and double-stained with uranyl acetate and lead citrate. Morphological observations were performed using a transmission electron microscope (HT7700; Hitachi, Tokyo, Japan) operating at 80 kV.

Statistical analysis

Results are expressed as mean ±SEM of the examined rats, for *in vivo* experiments, and mean ±SEM of multiple replicates, for molecular biology assays. Statistical analyses were performed using SPSS 22.0. Differences between two groups were analyzed using the unpaired two-tailed Student's *t*-test. Comparisons among multiple groups were performed using one-way ANOVA followed by Tukey's *post-hoc* test. A p-value <0.05 was considered statistically significant.

Results

Differences in SOCC expression in VSMCs and VECs

We compared protein and mRNA expression levels of SOCCs in VSMCs and VECs by Western blotting and RTqPCR, respectively. As expected, SOCCs were differentially expressed in VSMCs and VECs. Expression levels of STIM1, TRPC1, TRPC3, and TRPC5 (both protein and mRNA) were significantly higher in VSMCs than in VECs, whereas expression levels of NCX1, STIM2, Orai1, Orai2, TRPC4, and TRPC6 were lower. No differences were observed in NCX2 and Orai3 between the two cell types (Figure 1). These findings indicate that SOCC molecules are differentially expressed in VSMCs and VECs, which may contribute to their distinct effects on cell proliferation. Previous studies reported that knockout of STIM1 and Orai1 inhibited the proliferation of human umbilical vein endothelial cells (HUVECs),[8] while silencing TRPC1 suppressed high-glucose-induced proliferation and migration of retinal vascular endothelial cells.[9] Based on the literature and our experimental findings, STIM1 and Orai1 appear to inhibit endothelial cell proliferation, which was inconsistent with the aim of this study. Therefore, we selected TRPC3 and TRPC5 as candidate molecules for further investigation.

TRPC3/5 knockdown inhibited proliferation of VSMCs but not of VECs

TRPC3 is expressed in many cell types, with levels varying according to cell type, pathological condition, and disease.[10] TRPC5 can mediate store-operated calcium entry (SOCE) in smooth muscle cells by forming isoforms with TRPC1/6/7.[11] To confirm the effects of TRPC3/5 on VSMC and VEC proliferation, we knocked down TRPC3/5 expression in both cell types using adenoviral vectors. Successful depletion of TRPC3/5 was verified at the mRNA level (Figure 2A). A Cell Counting Kit-8 (CCK-8) assay revealed that VSMC proliferation was significantly inhibited from 48 h after TRPC3/5 knockdown, whereas VEC proliferation was not significantly affected up to 96 h (Figure 2B).

Cell cycle distribution was then analyzed by flow cytometry. In VSMCs, TRPC3 interference decreased the G_0/G_1 and S phases and increased the proportion of cells in the G_2/M phase compared with the non-silenced control (NSC) group. TRPC5 interference similarly reduced the G_0/G_1 and S phases, but G_2/M phase was unchanged, with an increased proportion of cells entering G_2/M. These findings suggest that silencing either TRPC3 or TRPC5 altered cell cycle distribution. Together with the CCK-8 results, these data indicate that TRPC3/5 knockdown arrested VSMCs in the G_2/M phase (Figure 2C). In contrast, TRPC3 or TRPC5 knock-

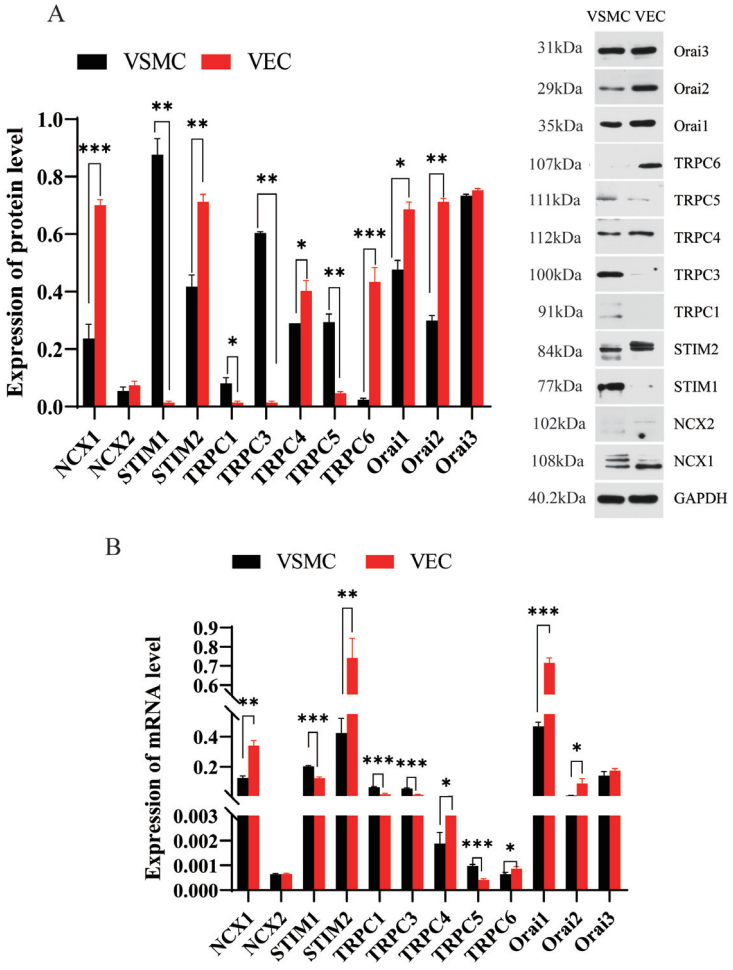

Figure 1. Expression levels of SOCCs in rat VSMCs and VECSSs. **A)** Western blot analysis of SOCC protein levels in rat VSMCs and VECSSs, showing representative immunoblots, with anti-GAPDH antibody as a control (right). **B)** Real-time-polymerase chain reaction' analysis of SOCC mRNA levels in rat VSMCs and VECSSs. Results expressed as mean + standard error of three experiments. *p< .05 *vs* VECSS, **p<0.01 *vs* VECSS, ***p<0.001 *vs* VECSS.

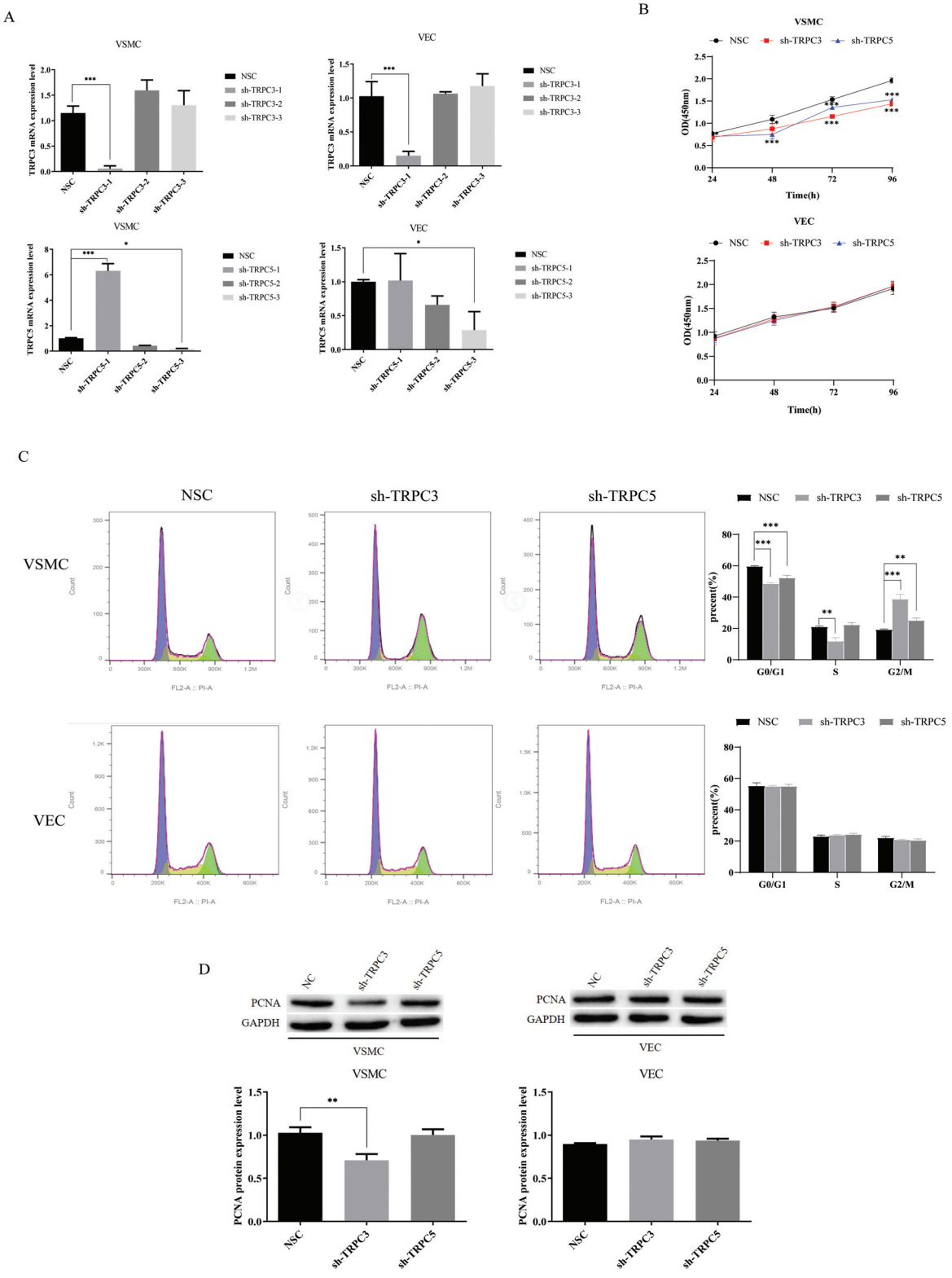

Figure 2. Effects of TRPC3/5 on VSMC and VECSS proliferation. **A)** VSMCs and VECSSs were infected with adenoviral particles (multiplicity of infection (MOI = 100) carrying sh-TRPC3 or sh-TRPC5 or control adenoviral particles (Ad. NSC) to select the adenovirus with the best interference efficiency (n=3). **B)** CCK-8 proliferation assay. VSMCs and VECSSs were infected with adenoviral particles (100 MOI) carrying sh-TRPC3 or sh-TRPC5 or Ad. NSC for 96 h. **C)** Cell cycle distribution was detected by flow cytometry; knockdown of TRPC3 in VSMCs decreased G_0/G_1 phase and S phase, and increased G_2/M phase, compared with the NSC group, while knockdown of TRPC5 decreased G_0/G_1 phase and G_2/M phase, but had no effect on S phase, compared with the NSC group, indicating that interfering with TRPC3 or TRPC5 blocked the cell cycle in G_2/M phase in VSMCs. **D)** Detection of PCNA protein expression by Western blot; knockdown of TRPC3 significantly decreased PCNA expression levels in VSMCs (n=5). *$p<0.05$ *vs* NSC, **$p<0.01$ *vs* NSC, ***$p<0.001$ *vs* NSC.

down did not significantly affect G_0/G_1, S, or G_2/M phases in VECs, suggesting no effect on their cell cycle progression. In addition, proliferating cell nuclear antigen (PCNA) expression was decreased in VSMCs with TRPC3 knockdown compared with the NSC group (Figure 2D). These results demonstrate that TRPC3/5 knockdown inhibited VSMC proliferation and induced G_2/M arrest, but had no significant effect on VEC proliferation.

TRPC3/5 knockdown inhibited thapsigargin-mediated Ca^{2+} influx by downregulating SOCC expression

It was next investigated whether the inhibitory effects of TRPC3/5 knockdown on VSMC proliferation were due to altered intracellular Ca^{2+} concentrations. Using Ca^{2+}-imaging technology, dynamic changes in intracellular Ca^{2+} were monitored. Intracellular Ca^{2+} stores were depleted with TG to activate SOCE, followed by restoration of extracellular Ca^{2+} concentration from 0 mM to 2 mM. Silencing TRPC3 or TRPC5 resulted in Ca^{2+} influx levels similar to those of the NSC group, but TG-induced Ca^{2+} influx was significantly reduced. In contrast, Ca^{2+} influx was only slightly decreased in VECs, and the difference was not statistically significant (Figure 3). These findings suggest that TRPC3/5 knockdown inhibited VSMC proliferation through downregulation of SOCE.

TRPC3/5 knockdown inhibited neointima formation in rats

A rat carotid artery balloon injury model was established, and adenoviral vectors were perfused into injured arteries to silence TRPC3/5 (sh-TRPC3, sh-TRPC5, NSC). In the balloon-injury group, neointima formation increased progressively, with greater smooth muscle cell proliferation and extracellular matrix deposition, confirming successful model establishment. Adenoviral vectors alone had no effect on blood vessels, indicating suitability for subsequent experiments. Rapamycin, a broad-spectrum anti-proliferative drug, inhibited proliferation of both VSMCs and VECs.[12,13] Consistent with previous studies,[14,15] the NSC+rapamycin group exhibited little to no neointima formation (Figure 4A). Importantly, silencing TRPC3 or TRPC5 significantly reduced neointimal area compared with the NSC group, without significantly affecting medial area. These results indicate that TRPC3 and TRPC5 contribute to neointima formation through regulation of VSMC proliferation, and that their knockdown effectively suppresses neointima development (Figure 4B).

TRPC3/5 knockdown had no effect on endothelial cell layer repair after vascular injury in SD rats

To evaluate endothelial cell layer repair, immunofluorescence was first used to locate the endothelial layer (Figure 5A). Endothelial cells were arranged in a monolayer under microscopy and were further identified by von Willebrand factor (vWF) immunohistochemistry (Figure 5B). At 14 days after injury, endothelial cell counts and repair percentages were higher in the sh-TRPC3 and sh-TRPC5 groups compared with the NSC+rapamycin group. No significant differences were observed between the sh-TRPC3 and sh-TRPC5 groups at either 7 or 14 days (Figure 5 C,D). Electron microscopy further confirmed that endothelial cells in the sh-TRPC3 and sh-TRPC5 groups sustained less damage compared

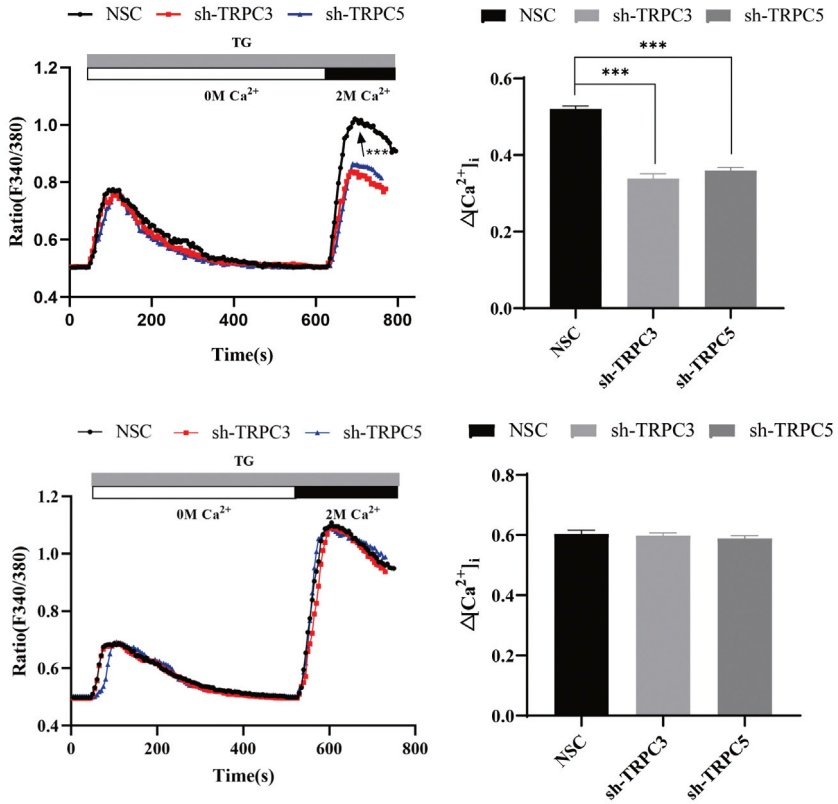

Figure 3. Changes in Ca^{2+} concentrations in VSMCs and VECSSs. TG was added to VSMCs and VECSSs to deplete the calcium pool, and the Ca^{2+} concentration was increased from 0 M to 2 M. Ca^{2+} concentration expressed as baseline fluorescence intensity (F; without TG and $CaCl_2$) at 340/380 nm, and change in Ca^{2+} concentration as $(F_{max}-F)/F$, where F_{max} is the peak fluorescence intensity (n=6). ***$p<0.001$ *vs* NSC.

with the NSC+rapamycin group at 14 days post-injury. In the rapamycin group, endothelial cells appeared elongated and spindle-shaped, with widened intercellular spaces, reduced tight junctions, and large areas of exposed elastic fiber. In contrast, endothelial cells in the TRPC3/5 knockdown groups were flat and spindle-shaped, with intact tight junctions, abundant fenestrations, and nearly complete endothelial coverage (Figure 5E). These results indicate that silencing TRPC3 or TRPC5 did not impair endothelial cell proliferation, and allowed endothelial repair to occur more rapidly than in both the NSC and rapamycin groups.

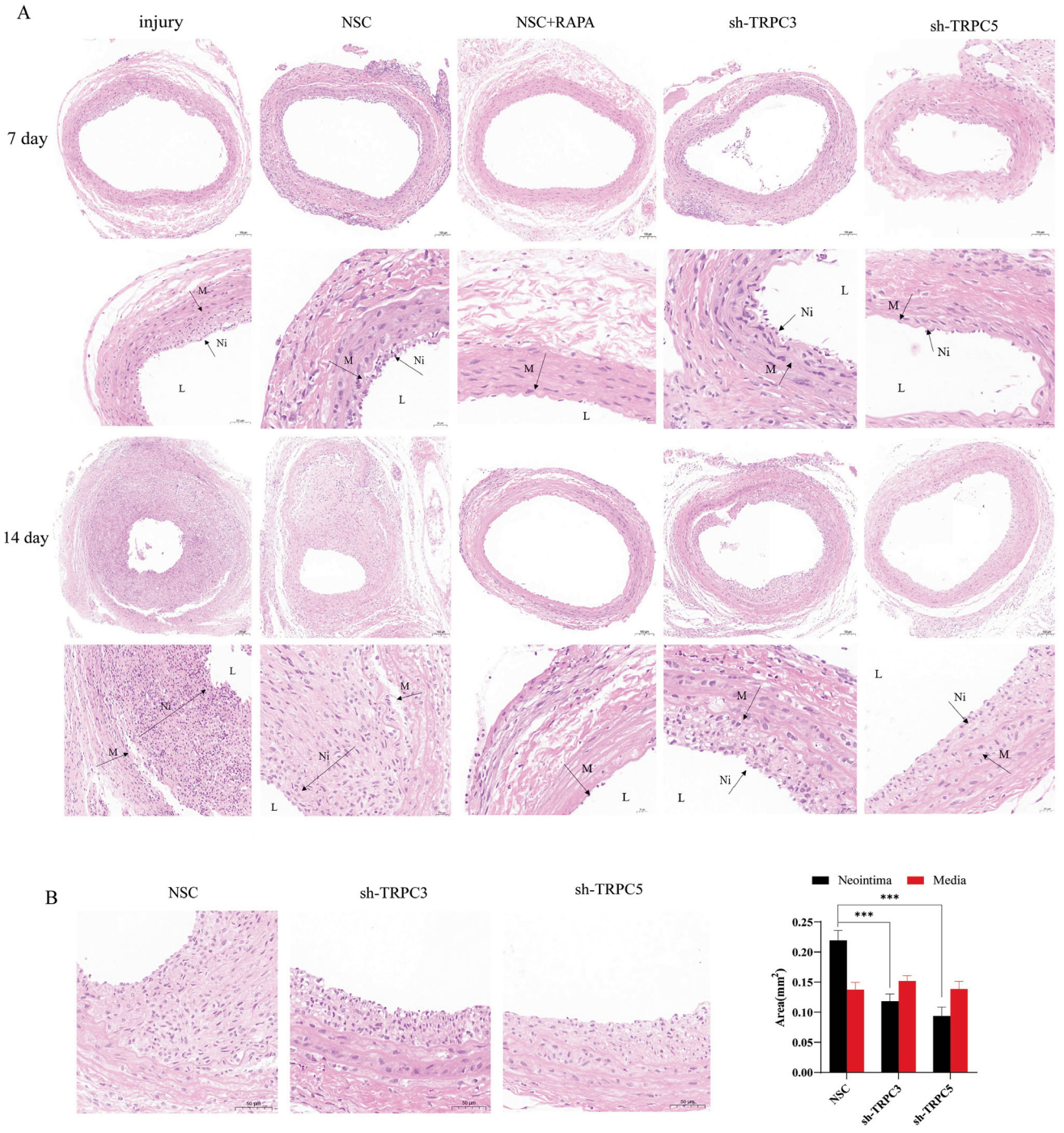

Figure 4. SD rats were sacrificed after 7 and 14 days and carotid artery sections were stained with hematoxylin and eosin. Neointima and media areas were compared among different adenovirus-transfection groups. **A)** Sections from balloon-injury, NSC, NSC+rapamycin, sh-TRPC3, and sh-TRPC5 transfection groups after 7 and 14 days; scale bars: 100 μm (100×) and 20 μm (400×). **B)** Sections from NSC, sh-TRPC3, and sh-TRPC5 transfection groups after 14 days; scale bars: 20 μm (400×). L, lumen; Ni, neointima; M, media (n=6). ***$p<0.001$ *vs* NSC.

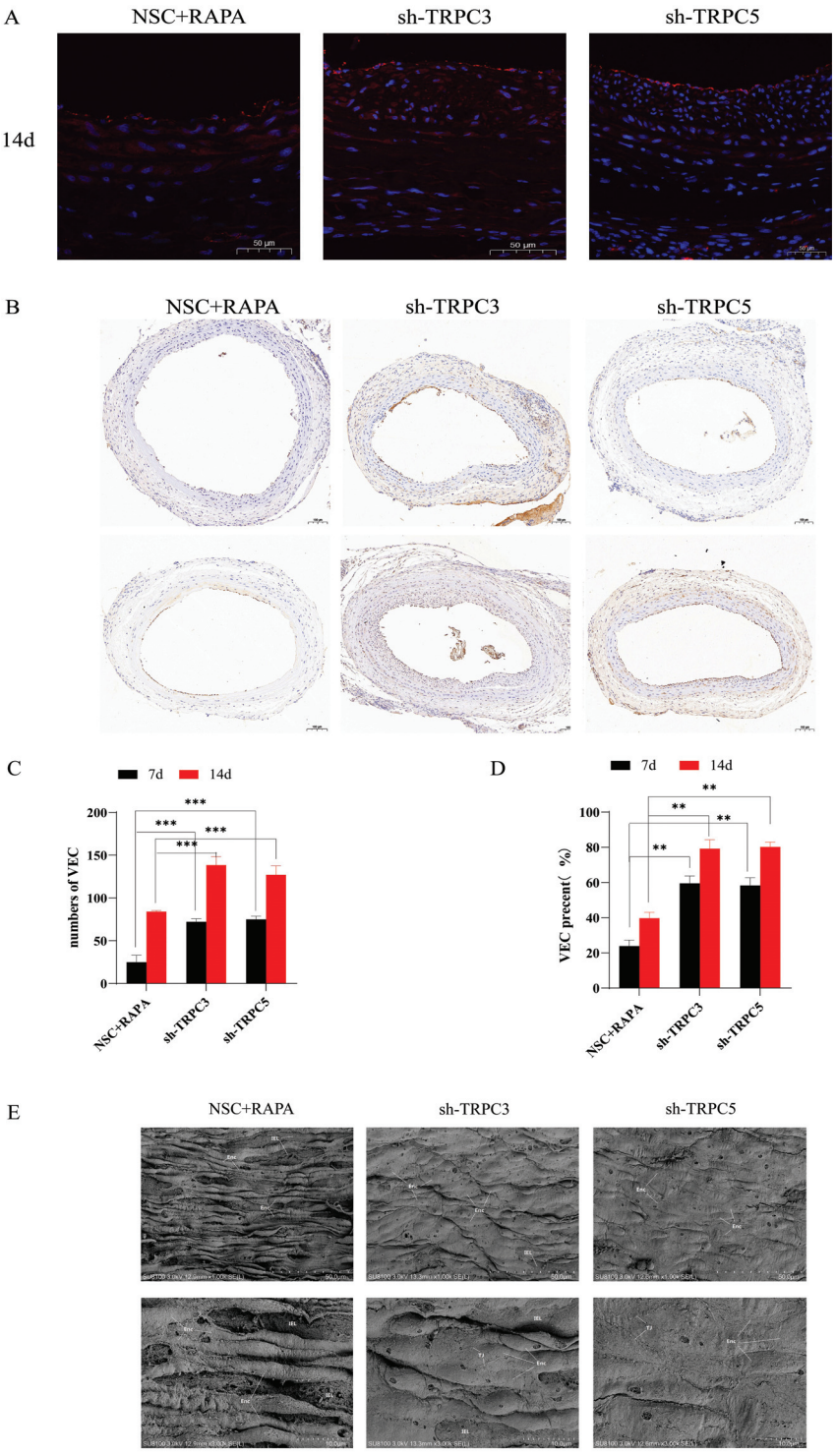

Figure 5. Endothelial cell repair after carotid artery injury in SD rats. **A)** Immunofluorescent localization of endothelial cell layer (200×) 14 days after transfection with adenovirus interference VECSstors; blue fluorescence, DAPI-stained nuclei; red fluorescence, vWF-positive endothelial cell layer; scale bars: 50 μm. **B)** Immunohistochemical detection of vWF in the endothelial cell layer 14 days after transfection with adenovirus interference VECSstors (100×); Nuclei stained blue; endothelial cell layer (vWF) stained brown; scale bars: 100 μm. **C)** Numbers of endothelial cells after transfection with different adenovirus interference VECSstors. **D)** Endothelial cell repair percentage after transfection with adenovirus interference VECSstors; endothelial cell repair percentage=endothelial cell proliferation length/vascular inner circumference. **E)** Morphology of endothelial cells in SD rat carotid artery examined by electron microscopy; NSC+rapamycin endothelial cells were long and spindle-shaped, with few fenestrations on the surface, widened intercellular spaces, and disappearance of tight junctions (TJ); The exposed underlying mesh-like elastic fiber layer (IEL) was relatively large and the surface was rough; the degree of damage to sh-TRPC3 and sh-TRPC5 endothelial cells was relatively low, the cells were spindle-shaped and flat, with fenestrations on the cell surface, abundant TJ, relatively complete endothelial cell coverage, and no obvious bare IEL; scale bars: 50 μm and 10 μm (n=6). ***p<0.001 *vs* NSC+rapamycin.

Discussion

In this study, we confirmed the important role of TRPC3/5 in cell proliferation using both *in vitro* and *in vivo* experiments. We provided the first evidence of differential expression levels of SOCC constituent molecules in VSMCs and VECs, highlighting the critical roles of TRPC3 and TRPC5 in VSMC proliferation. Expression of STIM, Orai, TRPC, and NCX varied between VSMCs and VECs, with TRPC3 and TRPC5 expressed at higher levels in VSMCs. We further demonstrated that knockdown of TRPC3 or TRPC5 suppressed TG-mediated Ca^{2+} entry and inhibited cell proliferation in VSMCs, but not in VECs. These findings were validated *in vivo*, as TRPC3/5 knockdown significantly reduced neointima formation in rat carotid arteries without impairing endothelial layer repair, showing superior reparative effects compared with rapamycin.

SOCE represents a key Ca^{2+} influx pathway, triggered by decreased Ca^{2+} concentrations in the ER.[16] Originally discovered in non-excitable cells, SOCE is now recognized as a mechanism operating in virtually all cell types, including excitable cells such as neurons and muscle cells. At the cellular level, SOCE regulates diverse physiological and pathological processes (Figure 6).

Previous evidence reported that ICRAC in HUVECs resembled that in RBL cells but with much lower magnitude, accompanied by reduced STIM1 protein levels in HUVECs. In HUVECs, Ca^{2+} influx was primarily mediated by STIM1 and Orai1, while TRPC1 and TRPC4 were not involved. These results suggest that the biological functions of SOCC molecules are cell type-dependent. Other studies[17-19] have also demonstrated interspecies and intercellular differences in SOCC-related molecule expression, helping to explain functional variability. In our study, higher TRPC3 and TRPC5 expression in VSMCs than in VECs provided the basis for subsequent proliferation studies.

TRPC channels are widely implicated in cell proliferation, and endothelial cell proliferation has been shown to be substantially inhibited by siRNA interference with TRPC1/4/6. However, the role of TRPCs remains controversial. For instance, TRPC1, the earliest identified family member, was discovered in human submandibular gland cells using patch-clamp techniques. Overexpression enhanced TG-induced Ca^{2+} entry, whereas TRPC1 knockdown reduced it.[20,21] In contrast, Sinkins *et al*.[22] reported that TRPC1 was not activated by store depletion in SF9 cells, as no increase in membrane currents was observed after TG treatment. Similarly, TRPC3 inhibition with siRNA in A431 cells significantly reduced SOCC activity,[23] while TRPC3 was found to participate in TG-mediated SOCE in HEK-293 cells.[24] These findings suggest that TRPCs may regulate intracellular Ca^{2+} levels through both SOCC-dependent and independent mechanisms. Our results indicate that silencing TRPC3 and TRPC5 inhibited VSMC proliferation by reducing SOCE-mediated Ca^{2+} influx and inducing G_2/M phase arrest, without exerting similar effects in VECs.

Different SOCC molecules contribute to Ca^{2+} influx *via* distinct pathways and participate in angiogenesis. For example, silencing STIM1 inhibited proliferation and migration of endothelial progenitor cells (EPCs) after vascular injury by regulating Ca^{2+} concentrations.[25] Similarly, TRPC1 knockdown suppressed EPC proliferation and migration, with evidence showing that TRPC1 forms a complex with STIM1 to co-regulate SOCE.[26] In our study, silencing TRPC3 or TRPC5 inhibited neointima formation after balloon injury, indicating that these channels are involved in this process. Furthermore, *in vivo* experiments showed that TRPC3/5 silencing had a more favorable effect on endothelial repair and regeneration than rapamycin.

In conclusion, our findings demonstrate that TRPC3 and TRPC5 promote VSMC proliferation and neointima formation by regulating SOCC-mediated Ca^{2+} influx, but have no significant effect on endothelial cell proliferation or endothelial repair. Silencing TRPC3 or TRPC5 was more effective than rapamycin, the commonly used drug-eluting stent coating. These results provide valuable insights for the development of novel drug-eluting stent strategies. Nonetheless, several limitations should be

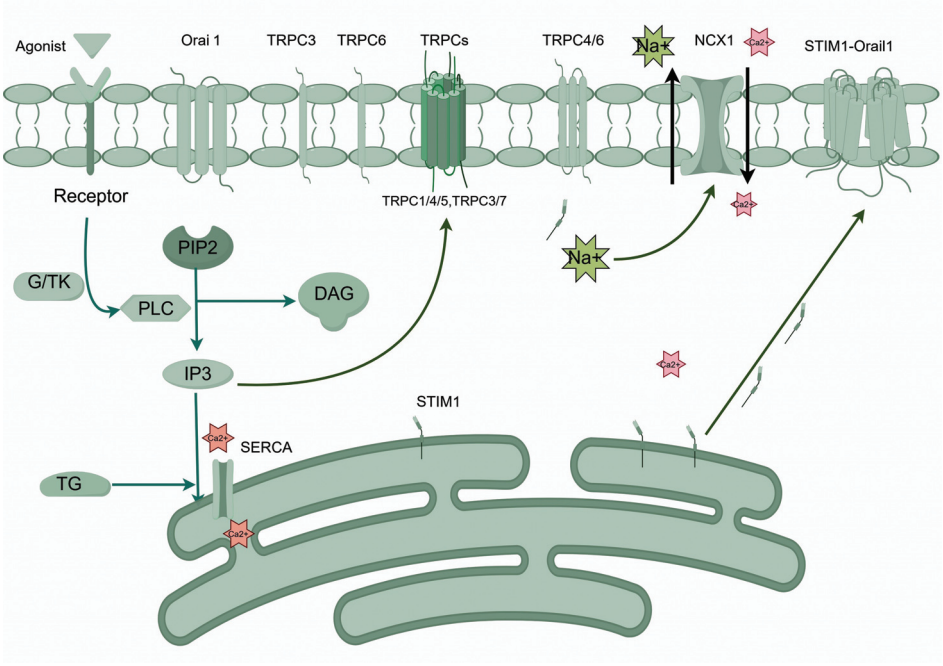

Figure 6. Schematic diagram of role of SOCE, showing the initiation process and interactions between constituent molecules. PM, plasma membrane; ER, endoplasmic reticulum; PLC, phospholipase C; PIP2:, phosphatidylinositol diphosphate; IP3, inositol triphosphate; DAG, diacylglycerol; TG, thapsigargin; SERCA,: sarcoplasmic reticulum Ca^{2+}-ATPase.

acknowledged. First, this study was performed in a rat model, and interspecies differences may limit the direct extrapolation of our findings to human physiology and clinical applications. Second, although TRPC3/5 silencing was verified at the mRNA level, it was not confirmed by Western blot analysis at the protein level; future studies should address this to strengthen the evidence for target specificity. Third, while TRPC3/5 knockdown effectively reduced neointima formation, potential off-target effects or compensatory pathways were not systematically evaluated, which may influence the interpretation of the results. Future investigations using human vascular tissues and more precise inhibition strategies are warranted to validate and extend these findings.

References

1. Akbari T, Al-Lamee R. Percutaneous coronary intervention in multi-vessel disease. Cardiovasc Revasc Med 2022;44:80-91.
2. Singh A, Zhang RS, Bangalore S. Percutaneous coronary intervention for heart failure due to coronary artery disease. Heart Fail Clin 2025;21:273-85.
3. Mathies M, Krieg EM, Mohr F, Zaradzki M, Wagner AH. Effects of rapamycin on the expression of redox enzymes in aortic vascular smooth muscle cells from Marfan syndrome mice. Pharmacology 2022;107:615-22.
4. Kuramitsu S, Sonoda S, Ando K, Otake H, Natsuaki M, Anai R, et al. Drug-eluting stent thrombosis: current and future perspectives. Cardiovasc Interv Ther 2021;36:158-68.
5. Liu X, Pan Z. Store-operated calcium entry in the cardiovascular system. Adv Exp Med Biol 2021;1349:303-33.
6. Prakriya M, Lewis RS. Store-operated calcium channels. Physiol Rev 2015;95:1383-436.
7. Wu Y, Shen L, Yin J, Chen J, Ge L, Ge J. 5 years of serial intravascular imaging outcomes of XINSORB sirolimus-eluting bioresorbable vascular scaffold. JACC Cardiovasc Interv 2019;12:602-3.
8. Gao X, Chen A, Tang H, Kong X, Zhang H, Wang Z, et al. m(6)A modification of Profilin-1 in vascular smooth muscle cells drives phenotype switching and neointimal hyperplasia via activation of the p-ANXA2/STAT3 pathway. Arterioscler Thromb Vasc Biol 2024;44:2543-59.
9. Wu B, Wu M, Yan P. Bioactive equivalent combinatorial components of Xiao-Xu-Ming decoction inhibit the calmodulin-mediated MLCK/MLC axis to attenuate coronary artery spasm. Phytomedicine 2025;142:156713.
10. Wang H, Cheng X, Tian J, Xiao Y, Tian T, Xu F, et al. TRPC channels: Structure, function, regulation and recent advances in small molecular probes. Pharmacol Therapeut 2020;209:107497.
11. Earley S, Brayden JE. Transient receptor potential channels in the vasculature. Physiol Rev 2015;95:645-90.
12. Li W, Li Q, Qin L, Ali R, Qyang Y, Tassabehji M, et al. Rapamycin inhibits smooth muscle cell proliferation and obstructive arteriopathy attributable to elastin deficiency. Arterioscler Thromb Vasc Biol 2013;33:1028-35.
13. Jang EJ, Bae IH, Park DS, Lee SY, Lim KS, Park JK, et al. Effect of a novel peptide, WKYMVm- and sirolimus-coated stent on re-endothelialization and anti-restenosis. J Mater Sci Mater Med 2015;26:251.
14. Stefanini GG, Holmes DJ. Drug-eluting coronary-artery stents. N Engl J Med 2013;368:254-65.
15. Durham AL, Speer MY, Scatena M, Giachelli CM, Shanahan CM. Role of smooth muscle cells in vascular calcification: implications in atherosclerosis and arterial stiffness. Cardiovasc Res 2018;114:590-600.
16. Lopez JJ, Jardin I, Sanchez-Collado J, Salido GM, Smani T, Rosado JA. TRPC channels in the SOCE scenario. Cells (Basel) 2020;9:126.
17. Vaeth M, Yang J, Yamashita M, Zee I, Eckstein M, Knosp C, et al. ORAI2 modulates store-operated calcium entry and T cell-mediated immunity. Nat Commun 2017;8:14714.
18. Eckstein M, Vaeth M, Aulestia FJ, Costiniti V, Kassam SN, Bromage TG, et al. Differential regulation of Ca(2+) influx by ORAI channels mediates enamel mineralization. Sci Signal 2019;12:eaav4663.
19. Zhang B, Liu B, Roos CM, Thompson MA, Prakash YS, Miller JD, et al. TRPC6 and TRPC4 Heteromultimerization mediates store depletion-activated NCX1 reversal in proliferative vascular smooth muscle cells. Channels 2018;12:119-25.
20. Liu X, Wang W, Singh BB, Lockwich T, Jadlowiec J, O'Connell B, et al. Trp1, a candidate protein for the store-operated Ca(2+) influx mechanism in salivary gland cells. J Biol Chem 2000;275:3403-11.
21. Liu X, Singh BB, Ambudkar IS. TRPC1 is required for functional store-operated Ca2+ channels. Role of acidic amino acid residues in the S5-S6 region. J Biol Chem 2003;278:11337-43.
22. Sinkins WG, Estacion M, Schilling WP. Functional expression of TrpC1: a human homologue of the Drosophila Trp channel. Biochem J 1998;331:331-9.
23. Kaznacheyeva E, Glushankova L, Bugaj V, Zimina O, Skopin A, Alexeenko V, et al. Suppression of TRPC3 leads to disappearance of store-operated channels and formation of a new type of store-independent channels in A431 cells. J Biol Chem 2007;282:23655-62.
24. Wu X, Babnigg G, Villereal ML. Functional significance of human trp1 and trp3 in store-operated Ca(2+) entry in HEK-293 cells. Am J Physiol Cell Physiol 2000;278:C526-36.
25. Cong XP, Wang WH, Zhu X, Jin C, Liu L, Li XM. Silence of STIM1 attenuates the proliferation and migration of EPCs after vascular injury and its mechanism. Asian Pac J Trop Med 2014;7:373-7.
26. Kuang CY, Yu Y, Wang K, Qian DH, Den MY, Huang L. Knockdown of transient receptor potential canonical-1 reduces the proliferation and migration of endothelial progenitor cells. Stem Cells Dev 2012;21:487-96.

Received: 14 August 2025. Accepted: 14 October 2025.

Licensee PAGEPress, Italy
European Journal of Histochemistry 2025; 69:4311
doi:10.4081/ejh.2025.4311